AtENO2 functions in the development of male gametophytes in *Arabidopsis thaliana*

Xiaofeng Ma[a], Yu Wu[a], Hainan Ming[a], Huimin Liu[a], Zijin Liu[a], Hongjie Li[b], Genfa Z hang[a*]

[a] Beijing Key Laboratory of Gene Resource and Molecular Development/College of Life Sciences, Beijing Normal University, Beijing 100875, China

[b] The National Engineering Laboratory of Crop Molecular Breeding/Institute of Crop Sciences, Chinese Academy of Agricultural Sciences, Beijing 100081, China

***** Correspondence: gfzh@bnu.edu.cn; Tel.: +86-18310076396

Abstract: Pollen fertility is an important factor affecting the seed setting rate and seed yield of plants. The *Arabidopsis thaliana* enolase gene *ENO2* (*AtENO2*) can affect the pollen morphology, germination, and pollen tube growth. *AtENO2* encodes two proteins AtENO2 and AtMBP-1. To examine the effect of AtENO2 protein on pollen development, the 2nd ATG of the *AtENO2* coding sequence for AtMBP-1 was mutated by site-directed mutagenesis, and transgenic plants expressing only AtENO2 but not AtMBP-1 were obtained. Phenotypic analysis indicated that AtENO2 was essential in the pollen development. The mechanisms of AtENO2 on pollen development were analyzed. AtENO2 can affect development of the pollen intine, and the mechanism may be that AtENO2 regulated the methyl esterification of pectin in pollen intine through ARF3 and AtPMEI-pi. The -734 ~ -573 sequence of *AtENO2* promoter is the main transcriptional regulatory region of AtENO2 affecting pollen development. The functional cis-acting element may be GTGANTG10(GTGA), and the trans-acting factors may be KAN, AS2 and ARF3/ETT. Moreover, the deletion of AtENO2 can cause significant difference in the expression of multiple genes related to pollen exine development. These results are useful for further studying the function of *AtENO2* and exploring the mechanism of plant pollen development.

Keywords: ENO2, MBP-1, PMEI, pectin, pollen intine, promoter

1. Introduction

Pollen development is a key step in double fertilization in flowering plants. Pollen fertility is a determinant of the seed setting rate and crop yield (Moles *et al*., 2005; Liu *et al*., 2016). In angiosperms, mature pollen is wrapped by a pollen wall, which ensures the maintenance of the normal structure and function of pollen, protects pollen from various environmental stresses and preserves pollen germination and polar growth of the pollen tube (Arizumi *et al.*, 2004; Scott *et al.*, 2004; Guan *et al.*, 2008). The pollen wall is one of the most complex cell walls among all plant cell wall types. It is divided into the exine and intine layers. The main components of the intine layer include cellulose, hemicellulose, pectin, and structural protein; these components are similar to those of common cell walls (Quilichini *et al.*, 2015; Hesse *et al.*, 2016; Gigli *et al.*, 2018). As a major component of the pollen intine, pectin is closely related to formation of the pollen wall and growth of the pollen tube (Varner *et al*., 1989; Aouali *et al*., 2001; Dardelle *et al*., 2010). A large number of pectin metabolism-related genes, including genes encoding pectin methylesterase (PME), pectin methylesterase inhibitor (PMEI), polygalacturonase (PG), and pectate lyase like

(PLL), are involved in construction of the pollen intine.

Abnormal pectin synthesis and modification processes directly influence intine formation (Ridley *et al*., 2001; Willats *et al*., 2001). During pectin metabolism, PMEs can catalyze pectin demethyl esterification, and demethyl esterified pectin is degraded by PG and pectate lyase (Bosch *et al.*, 2005). Demethyl esterified pectin combines with calcium ions to form Ca^{2+}-pectinate crosslinking complexes, which can enhance cell wall hardness (Pelloux *et al*., 2007; Mohnen *et al*., 2008; Chebli *et al*., 2012). At the top of pollen tube, the cell wall is only composed of the pectin layer. Demethyl esterified pectin is distributed mainly in the shank region of the pollen tube and is able to maintain the hardness of the pollen tube wall. Methyl esterified pectin is located mainly in the top region of the pollen tube to improve plasticity of the pollen tube tip (Bosch *et al*., 2005; Chebli *et al*., 2012). The enzymatic activity of PME is negatively regulated by PMEI, which can bind with the active site of PME to form a 1:1 complex (Zhang *et al*., 2010; Woriedh *et al*., 2013; Paynel *et al*., 2014). Pectin methylesterase inhibitor was first found in *Actinidia chinensis* Planch (Giovane *et al*., 2004; Matteo *et al*., 2005). Transcripts of PMEI are abundant in different tissues, developmental stages, and stress responses of plants (Pinzón-Latorre *et al*., 2013; Nguyen *et al*., 2016). Several PMEI genes, including *AtPMEI1*, *AtPMEI2*, *AtPMEI3*, *AtPMEI6*, *AtPMEI10*, *AtPMEI12*, *EDA24*, *BcMF23*, and *ZmPMEI1*, have been cloned (Peaucelle *et al*., 2008; Zhang *et al*., 2010; Saez-Aguayo *et al*., 2013; Lionetti *et al*., 2017; Liu *et al*., 2018a).

Enolase (ENO, 2-phospho-D-glycerate hydrolyase), a metalloenzyme in glycolysis, can catalyze the dehydration of 2-phospho-D-glycerate (2-PGA) to phosphoenolpyruvate (PEP). ENO2 is an isozyme of ENO that is widely distributed and highly conserved in plants. *ENO2* not only participates in the glycolysis process but also has many other functions. One of its functions is to regulate the growth and development of plants. Compared with wild-type (WT) *Arabidopsis*, the T-DNA insertion mutant *eno2*$^{-}$ (*los2-2*, SALK-021737) was found to exhibit many phenotypic defects. The morphology of *eno2*$^{-}$ pollen was shrunk and deformed, the pollen germination rate *in vitro* was significantly decreased, and the pollen tube length was reduced. These defects led to a decrease in the seed setting rate in *eno2*$^{-}$ (Eremina *et al*., 2015; Liu *et al*., 2019, 2020). However, the molecular mechanism of *AtENO2* in pollen development is still unclear.

AtENO2 encodes both an enolase (AtENO2) protein and a c-Myc binding protein 1-like (AtMBP-1) protein. AtENO2 is 444 amino acids in length. AtMBP-1 is translated from the second start codon of *AtENO2* transcripts and lacks 92 amino acids in the N-terminus of AtENO2. There is a typical enolase structure (from the 3rd to the 139th amino acid) in the N-terminus of AtENO2, resulting in the loss of enolase activity in AtMBP-1 (Lee *et al*., 2002; Kang *et al*., 2013). *Arabidopsis* transgenic plants that overexpress *AtMBP-1* (in the *WT/35S::AtMBP-1-GFP* line) show defects similar to those of *eno2*$^{-}$, and AtMBP-1 is modulated by the E3 ubiquitin ligase AtSAP5 (Kang *et al*., 2013). AtMBP-1 has been found to exert negative feedback regulation on the promoter of *eno2*$^{-}$ (Eremina *et al*., 2015). The *eno2*$^{-}$*/35S::AtENO2-GFP* line can return to the WT morphology, but the *eno2*$^{-}$*/35S::AtMBP-1-GFP* line cannot (Liu *et al*., 2019). However, the function of AtENO2 in plant growth and development has not been fully characterized.

In this work, we observed that AtENO2 was able to regulate the pollen development and morphology, especially the pollen wall. The mechanism of AtENO2 affecting pollen intine may be related to ARF3 and AtPMEI-pi, which are associated with formation of the pollen intine by regulating pectin methyl esterification in pollen grains. The objectives of this study were to explore the function and regulatory mechanism of *AtENO2* on pollen development.

2. Materials and methods

2.1. Plant materials and growth conditions

The WT *Arabidopsis* is the ecotype Columbia (Col-0), and the mutant AtENO2 T-DNA insertion (SALK_021737) was provided by the *Arabidopsis* Biological Resource Center (ABRC, Columbus, Ohio). The homozygous *eno2*$^{-}$*/35S::mAtENO2-GFP* line was obtained by screening on Murashige and Skoog (MS) medium supplemented with 50 mg/mL hygromycin. The seeds were sterilized with 0.1% (w/v) $HgCl_2$ for 5 min and washed 3 times with sterilized water. They were sown on solid MS plates and vernalized at 4°C for 2 d in the dark. The 10-day-old seedlings were transplanted into soil and grown in a growth chamber at 22°C with a 16-h light/8-h dark cycle and a relative humidity of 70%.

2.2. Plasmid construction

Using the WT *Arabidopsis* cDNA as a template, the coding sequence of *AtENO2* was cloned with primers 5'-GTCCTAGGATGGCTACTATCACCG-3' and 5'-CCCATGGGGTAGGGTTCCACAGGTT-3' and transformed into the pEASY-T3 vector (TransGen, Beijing, China). Then, using the *pEASY-T3-AtENO2* plasmid as a template and 5'-CTGCTATTGACAACTTCCTGGTCCATGAAC-3' and 5'-GGAAGTTGTCAATAGCAGTCTGCTGAGTTG-3' as primers, site-directed mutagenesis was carried out using a Fast Mutagenesis System (TransGen, Beijing, China). Positive clones were identified to obtain the plasmid *pEASY-T3-mAtENO2.* The coding sequence of *mAtENO2* was cloned using the plasmid *pEASY-T3-mAtENO2* as a template and transformed into the *pCAMBIA1302* vector to generate the construct vector *35S::mAtENO2-GFP*, which encodes only mAtENO2. This construct vector was delivered into the *eno2*$^{-}$ *Arabidopsis* plants via the *Agrobacterium* tumefaciens-mediated transformation system, resulting in two homozygous transgenic lines, *eno2*$^{-}$*/35S::mAtENO2-GFP-5* (*mAtENO2-5*) and *eno2*$^{-}$*/35S::mAtENO2-GFP-8* (*mAtENO2-8*).

2.3. Quantitative real-time RT-PCR analysis

Total RNA was isolated using an Eastep® Super Total RNA Extraction Kit (Promega, Madison, Wisconsin, USA) and reverse transcribed using a GoScript™ Reverse Transcription system (Promega). Quantitative real-time RT-PCR (qRT-PCR) was performed using a TransStart® Green qPCR SuperMix Kit (TransGen, Beijing, China). Reactions were performed at 94°C for 30 s, 40 cycles at 94°C for 5 s, and at 60°C for 34 s. The expression of β-actin was measured in parallel as an endogenous control. The qRT-PCR experiments included three independent biological replicates and three technical replicates for each biological replicate. The primers used for qRT-PCR are shown in Table S1.

2.4. Enolase activity assay

Enolase activity was determined using an ultraviolet and visible spectrophotometer (Straeten *et al*., 1991). The reactions were performed in 50 mM Tris-HCl (pH 7.5) containing 1 mM $MgCl_2$ and 2.5 mM 2-phospho-D-glycerate. The reaction mixture was incubated at 25°C for 10 min, and 2 mL HCl (0.1 M) was added to terminate the reaction. The absorbance of the sample at 230 nm was

measured. The experiment consisted of three independent biological replicates.

2.5. High-throughput mRNA sequencing analysis

Total RNA was extracted from the 45-day-old *Arabidopsis* plants, RNA concentration was quantified using Qubit® 3.0 Flurometer (Life Technologies, CA, USA) and RNA integrity was assessed using RNA Nano 6000 Assay Kit on the Agilent Bioanalyzer 2100 system (Agilent Technologies, CA, USA). The cDNA library construction and sequencing were performed by Annoroad Genomics (Beijing, China) on the Illumina Hiseq Xten platform (Illumina, San Diego, CA, USA). The insert size of cDNA library was detected by Agilent 2100 (Agilent Technologies, CA, USA). Gene expression levels were assessed using Fragments per Kilobase per Million Mapped Fragments (FPKM). HTSeq2 was used to calculate the raw read counts for each gene. Gene expression normalization among samples was performed using DESeq2. The screening criteria was FC (Fold change)≥2 and q≤0.05. Genes function were annotated based on the Gene ontology (GO, http://www.geneontology.org/) and Kyoto Encyclopedia of Genes and Genomes (KEGG, https://www.genome.jp/kegg/) databases.

2.6. Pectin methylesterase activity assays

Arabidopsis seedlings were ground and infused with a protein-extracting solution. The reactions were performed on ice for 30 min and then centrifuged for 15 min at 4°C and 12000 rpm. The supernatant was used to measure the protein concentration using the BCA Protein Assay Kit (Sangon Biotech, Shanghai, China). A chromogenic solution (0.5% pectin, 0.2 M NaCl, and 0.015 (w/v) methyl red , pH 6.8) (950 μL) was added to 20 μL protein solution, and the absorbance was detected at 525 nM after 20 min of reaction. The standard curve was measured with 0.01 M HCl, and the activity of PME was expressed by the number of H^+ released per hour per unit mg protein (Solecka *et al*., 2008; Dedeurwaerder *et al*., 2009).

2.7. *In vivo* determination of pollen viability

Pistils of *Arabidopsis* were fixed and decolorized in a solution consisting of 10% ethanol, 30% chloroform, and 60% acetic acid, immersed in 4 mol/L NaOH for 40 min and washed with 50 mM/L K_3PO_4 (pH 7.5) 3 times. After staining with aniline blue for 15 min, the pistils were observed under a fluorescence microscope ImagerM1 (Carl Zeiss AG, Oberkochen, Germany).

2.8. Transmission electron microscopy

Anthers collected at 10-13 developmental stages (Sanders *et al.,* 1999) were immersed in 2.5% glutaraldehyde (v/v) in 0.1 M phosphate buffer (pH 7.2), fixed at 4°C, and washed with 0.1 mol/L phosphate buffer (pH 7.2) for 3 × 15 min and with 1% osmic acid solution for 2 h. The anthers were then washed with 0.1 mol/L phosphate buffer (pH 7.2) for 3 × 15 min. The samples were dehydrated with a gradient ethanol solution series (i.e., 50, 70, 80, 90, and 95%) for 15 min each. Then, the samples were treated with 100% ethanol for 20 min, acetone for 20 min, a mixture of Spurr embedding agent and acetone (1:1) for 1 h, and a mixture of embedding agent and acetone (3:1, v/v) for 3 h. The samples were embedded in resin and heated at 70°C overnight to obtain the embedded samples. Sections were sliced with an EMUC7 instrument (Leica, Wetzlar, Germany), stained with uranyl acetate and lead citrate for 5-10 min, and observed under an HT7800 transmission electron microscope (HITACHI, Tokyo, Japan) (Zhang *et al*., 2007).

2.9. β-Glucuronidase (GUS) activity assay

GUS protein fusion expression vectors were constructed for each truncated sequence of the *AtENO2* promoter and transformed into WT *Arabidopsis* to obtain homozygous transgenic lines. Flowers of the transgenic and WT plants were incubated at 37°C overnight in GUS solution comprising 1 M PBS buffer (pH 7.0), 40 mM potassium ferricyanide, 40 mM potassium ferrocyanide, 0.1 M EDTA, and 5 mg/mL X-Gluc. The samples were decolorized in 70% ethanol. Photographs were taken using a Zeiss DiscoveryV12 fluorescence microscope.

2.10. Yeast One-Hybrid Assay

Yeast one-hybrid assay was performed according to the Matchmaker® Gold Yeast One-Hybrid Library Screening System (Clontech, CA, USA). The tandem repeat of the -734 ~ -573 sequence of *AtENO2* promoter was synthesized by Sangon Biotech (Shanghai, China). Arabidopsis transcription factor library was constructed by Oebiotech (Shanghai, China). The bait vector was transformed into the yeast strain AH109. The transcription factor library was in the yeast strain Y187. After the two transformed strains were mixed cultured, the transcription factors interacting with DNA were screened on the synthetic dextrose medium-Trp-Ura, -His-Trp-Ura, and -Trp-Leu-Ade-His.

3. Results

3.1. Identification of the mAtENO2 line with a mutation in the 2nd ATG

AtENO2 encodes AtENO2 and AtMBP-1 with the 1st ATG and the 2nd ATG as initiator codons, respectively. AtMBP-1 lacks the N-terminal amino acid of AtENO2 (Fig. 1A). To examine the functions of AtENO2 in pollen development, the 2nd ATG of the *AtENO2* coding sequencing was mutated to CTG (Leu) by site-directed mutagenesis. The mutated *AtENO2* coding sequence only encodes AtENO2 (mAtENO2). A vector was constructed to contain the coding sequence of mAtENO2 that was fused at their C-terminus to the GFP coding sequence under transcriptional control of the *CaMV 35S* promoter. The construct vector (*35S::mAtENO2-GFP*) was transformed into *eno2*$^{-}$ *Arabidopsis* plants (Fig. 1B), resulting in two homozygous transgenic lines, *eno2*$^{-}$*/35S::mAtENO2-GFP-5* (*mAtENO2-5*) and *eno2*$^{-}$*/35S::mAtENO2-GFP-8* (*mAtENO2-8*). The expression of *AtENO2* was significantly higher in the *mAtENO2-5* and *mAtENO2-8* lines than in the *eno2*$^{-}$ line. The expression of *AtENO2* was higher in the transgenic plants than in the WT (Fig. 1C). The enolase activity of AtENO2 was similar in the *mAtENO2-5* and *mAtENO2-8* transgenic plants compared to WT (Fig. 1D).

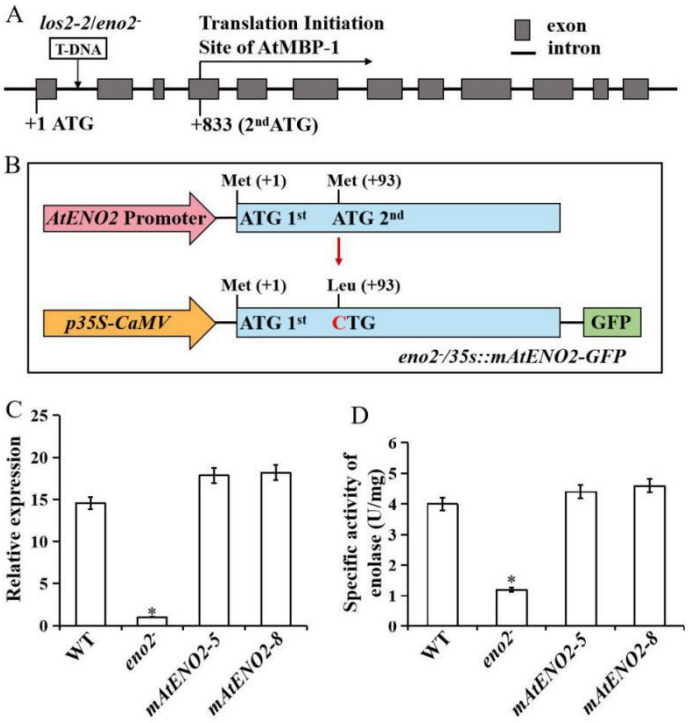

Fig. 1. Schematic representation of the mAtENO2 mutation and identification of the transgenic lines. (A) Intron-exon organization of the *AtENO2*. The position of the T-DNA insertion in the *eno2*$^{-}$ mutant alleles and the initiator codon ATG of coding AtENO2 and AtMBP-1 is indicated. (B) Schematic representation of vector construction. The initiator codon 2nd ATG of the *AtENO2* coding sequence was mutated to CTG by site-directed mutagenesis. Orange and green boxes indicate the *CaMV 35S* promoter and GFP, respectively. (C) Relative expression levels of *AtENO2* and (D) enolase activity of AtENO2 in the WT, *eno2*$^{-}$, *mAtENO2-5*, and *mAtENO2-8* lines. All experiments were performed in triplicate. Asterisks indicate a significant difference from the WT ($P < 0.05$).

3.2. Functions of AtENO2 in pollen development of *Arabidopsis*

The internal morphology of flowers in the same period was observed. Compared with the WT, *mAtENO2-5*, and *mAtENO2-8* lines, in *eno2*$^{-}$ mutant plants, stamen development was impaired, the filaments became shorter, and there were few pollen grains on the stigmas and in the anthers (Fig. 2A). The pollen vigor experiment *in vivo* showed stronger pollen-stigma binding and pollen germination abilities of *mAtENO2-5* and *mAtENO2-8* lines than the WT and *eno2*$^{-}$ (Fig. 2B). Compared with WT plants, the pollen development of *eno2*$^{-}$ was defective, and the pollen morphology was shrunken and deformed. However, the pollen phenotype of the *mAtENO2-5* and *mAtENO2-8* lines were similar to that of the WT (Fig. 2C). Based on the Alexander staining experiment, the defective pollen in the *eno2*$^{-}$ plants was also viable (Fig. 2D), which indicated that AtENO2 had no significant effect on pollen viability. Therefore, the defects of pollen morphology, germination and pollen tube growth in *eno2*$^{-}$ mutant may be related to the pollen wall. We found that the silique phenotype of *mAtENO2-5* and *mAtENO2-8* lines were identical to that of the WT, while the silique of *eno2*$^{-}$ was shorter than that of the WT, and there were fewer seeds in siliques of *eno2*$^{-}$ than in the WT (Fig. 2E).

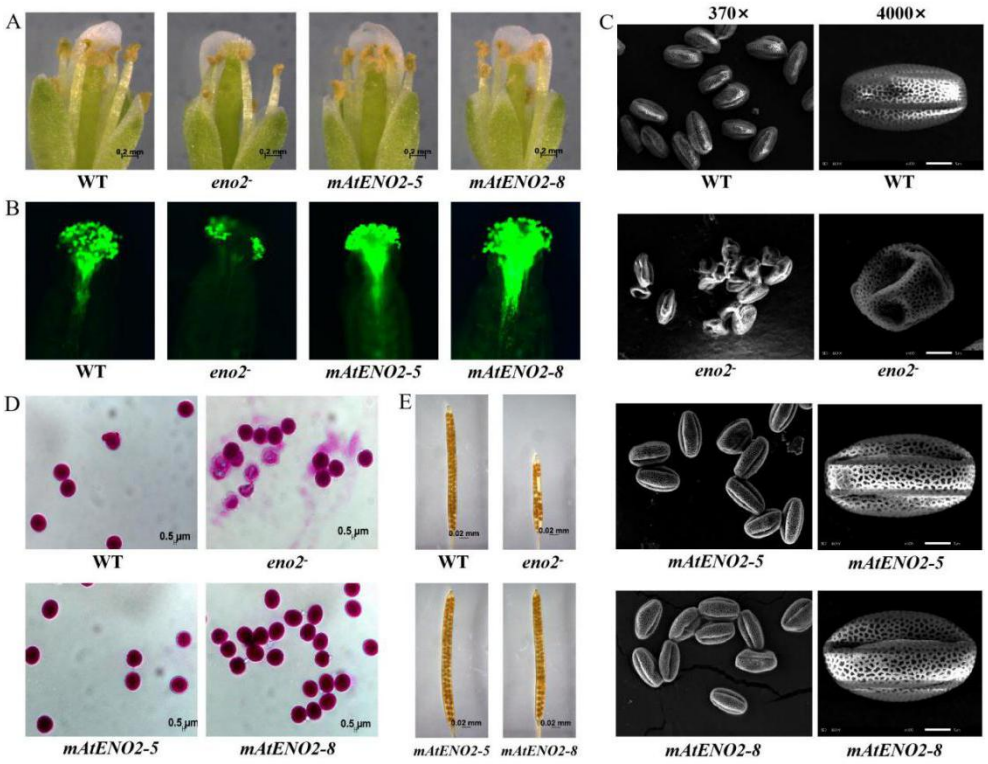

Fig. 2. Functions of AtENO2 on pollen development and morphology. (A) Comparison of stamen development of flower. (B) Aniline blue stained pollen and pollen tube on the stigma *in vivo*. (C) Transmission electron micrographs of pollen grains. (D) Alexander staining experiments of pollen grains. (E) Comparison of silique length and seeds in siliques observed under transparency. Plants were randomly selected and photographed under the same conditions.

3.3. Transcriptome analysis of the WT, *eno2*$^{-}$, and *mAtENO2-8* lines

The percentages of clean reads for the WT, *eno2*$^{-}$, and *mAtENO2-8* plants to the *Arabidopsis* genome sequences were 96.59%, 96.8%, and 97.41%, respectively. There were 2562 differentially expressed genes (DEGs), 1420 up-regulated and 1142 down-regulated, between the *eno2*$^{-}$ mutant and WT (*eno2*$^{-}$ vs. WT) (Fig. 3A). As shown in Fig. 3B, 1436 DEGs were identified from *mAtENO2-8* and *eno2*$^{-}$, 592 of which were up-regulated and 844 were down-regulated. A total of 2849 DEGs were identified from *mAtENO2-8* vs. WT, of which 1468 genes were up-regulated and 1381 genes were down-regulated (Fig. 3C). Among them, 147 were differentially expressed in the three groups. We found that these 1340 genes should be mainly related to AtMBP-1 by analyzing the variables of the three groups (Fig. 3D). At the transcriptional level, the DEGs were clustered according to the gene expression level. There were significant differences among the WT, *eno2*$^{-}$, and *mAtENO2-8* lines (Fig. 3E). To understand the function of DEGs, we performed GO annotations analysis (Table 1). In the *mAtENO2-8* vs. *eno2*$^{-}$, there were 47 GO terms that were significantly changed at FDR < 0.05, including 20 biological processes, 12 cellular components, and 10 molecular functions (Fig. 3F). The top term was “cell part” (265 up-regulated and 408 down-regulated DEGs) in the cellular component category. The top term was “cellular process” (239 for up-regulated DEGs, 366 for down-regulated DEGs) in the biological process category. In the molecular function category, the highest GO term for DEG count was “binding” (197 up-regulated and 324 for down-regulated DEGs) (Table S2). To further explore the biological

functions of the DEGs, an enrichment analysis based on KEGG database was performed. The KEGG analysis showed that 677 DEGs were enriched in 106 pathways in *eno2*$^{-}$ vs. WT group, 701 DEGs were enriched in 110 pathways in *mAtENO2-8* vs. WT group, and 355 DEGs were enriched in 89 pathways in *mAtENO2-8* vs. *eno2*$^{-}$ group. Among the comparison groups, phenylpropanoid biosynthesis had the greatest number of DEGs (Table S3, 4, 5). The expression profiles of 15 selected DEGs (5 up-regulated and 10 down-regulated) from the RNA-seq assay were confirmed by qRT-PCR. The expression of these genes was consistent in the qRT-PCR and RNA-seq analyses (Fig. 3G). The Pearson correlation coefficient of the gene expression by the two techniques was 0.709 ($P < 0.01$), indicating the reliability of the RNA-seq data.

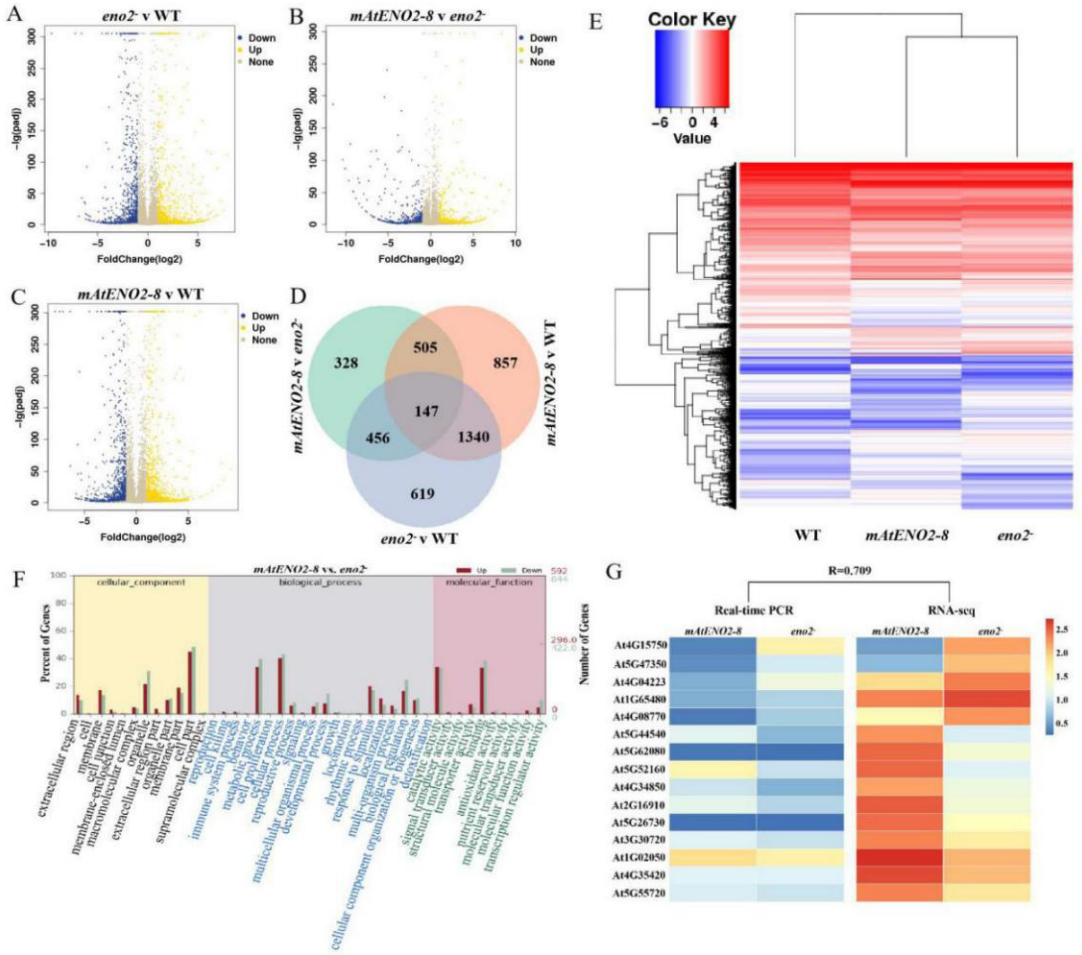

Fig. 3. Analysis of differentially expressed genes (DEGs) for the WT, *eno2*$^{-}$ mutant, and *mAtENO2-8* line. Volcano maps of the DEGs for *eno2*$^{-}$ vs. WT (A), and *mAtENO2-8* vs. *eno2*$^{-}$ (B), and *mAtENO2-8* vs. WT (C). Blue and yellow dots denote significantly different expression levels in each data set (fold change > 2, $P < 0.05$). Gray dots indicate no significant difference in the expression of genes. (D) Venn diagram showing the number of DEGs shared between comparison groups. (E) Heatmap of the DEG expression level. Each row represents a gene, and each column represents a sample. (F) GO analysis of DEGs in the group *mAtENO2-8* vs. *eno2*$^{-}$. (G) RNA-seq results were examined by qRT-PCR with three biological replicates. The relative expression is represented by the color scales as indicated on the right. *R* is the Pearson's correlation coefficient value between the two methods.

Table 1 The count of total and significantly enriched Gene Ontology.

Comparison groups	Functional classification of DEGs			GO with significant enrichment		
	Biological Process	Cellular Component	Molecular Function	Biological Process	Cellular Component	Molecular Function
eno2^{-} vs. WT	2744	414	1110	149	11	63
mAtENO2-8 vs. WT	2942	455	1171	124	18	66
mAtENO2-8 vs. *eno2*$^{-}$	2176	332	826	50	15	22

3.4. Analysis of differentially expressed genes related to pollen development

To analyze the mechanism of pollen development regulated by AtENO2, the DEGs related to pollen in the comparison group of *mAtENO2-8* vs. *eno2*$^{-}$ were analyzed. There were 14 sub-category classification of DEGs related to pollen (Table 2). These functions were mainly related to the formation of pollen wall, pollen recognition, pollen germination and pollen tube development, which indicates that AtENO2 may play an important role in development of the pollen wall and pollen tube growth. There were 44 DGE associated with pollen wall and pollen tube and cluster analysis of these DEGs was performed (Table S6). As shown in Fig. 4A, *AMS*, *MS1*, *ABCG1*/*26*, *CYP703A2*, *CYP704B1*, *PKSA*/*B* and *TKRP1*/*2* are all important genes involved in regulation of the pollen exine and pollen coat formation (Kim *et al*., 2010; Chen *et al*., 2011; Zhu *et al*., 2020). *VGDH2* and *PME48* are pollen specific expression genes belonging to *PMEs* family. They are essencial to pollen germination and pollen tube growth (Jiang *et al*., 2005; Leroux *et al*., 2015). Pectin is the main component of pollenintine. Therefore, AtENO2 may also affect the development of pollen intine.

Among the DEGs of *mAtENO2-8* vs. *eno2*$^{-}$, *At4G15750* gene (Log2FC=6.572) was the most significantly up-regulated gene, but it was not annotated into GO function. According to the Tair database (https://www.arabidopsis.org), *At4G15750* encodes a pectin methylesterase inhibitor superfamily protein. There were 79 *PMEI* family genes in *Arabidopsis* (Table S7). Phylogenetic analysis showed that *At4G15750* belonged to a branch of *PMEIs* family and it's amino acid sequence of was similar to those of *At3G12880* and *At1G56100*, but the specific functions of these genes have not been reported (Fig. 4B). The amino acid sequence of *At4G15750* was conserved in the *Arabidopsis* PMEI family, especially the three cysteine residues that could form the secondary structure by forming disulfide bonds (*) were conserved (Fig. 4C). Analysis of the tertiary structure of *At4G15750* coding product showed that it had pectin methylesterase inhibitory activity, and its tertiary structure was 100% similar to the sequenced PMEI proteins (Fig. 4D). According to the Tair database, the *At4G15750* gene was expressed during mature pollen stage, flowering stage, plant embryo globular stage, and expressed in flower pedicel, plant embryo, plant sperm cell, pollen, sepal. Therefore, the *At4G15750* may be related to the mechanism of pollen development regulated by AtENO2. According to the main functional orientation of pectin in pollen is pollen intine, the *At4G15750* gene was named *AtPMEI-pi*.

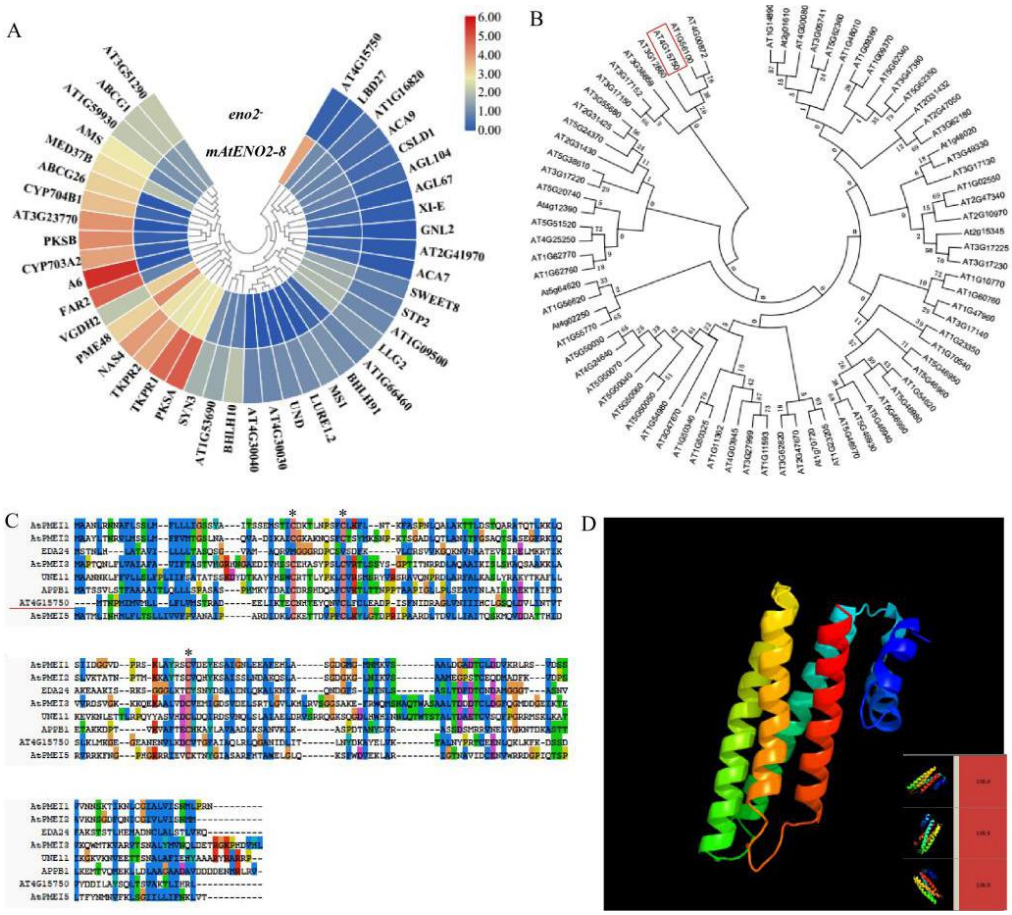

Fig. 4. Analysis of DEGs related to pollen development. (A) Heatmap showing the relative expression level of major DEGs related to pollen development. (B) Phylogenetic tree of the PMEI family in *Arabidopsis*. Amino acid sequences of PMEI family proteins were analyzed by the neighbor-joining method with genetic distance calculated by MEGA4.1. The numbers at the nodes represent percentages. The red box indicates *AtPMEI-pi*. (C) Sequence alignment of AtPMEI-pi with known PMEIs in *Arabidopsis*. The asterisk indicate the cysteine residues. (D) The tertiary structure of AtPMEI-pi was analyzed by Phyre2.

Table 2 Functional classification of the DEGs related to pollen.

GO category	Up-regulated DEGs	Down-regulated DEGs	Total	Percentage* (%)
Pollen wall assembly	2	12	14	33.3
Pollen exine formation	1	10	11	33.3
Pollen hydration	4	0	4	66.7
Pollen development	7	10	17	10.1
Pollen sperm cell differentiation	1	4	5	20
Pollen maturation	2	1	3	13.6
Pollen germination	3	1	4	10.3
Recognition of pollen	4	1	5	8
Pollen tube growth	2	4	6	6.7
Regulation of pollen tube growth	2	0	2	7.7
Pollen tube guidance	0	2	2	5.1

Pollen coat	6	0	6	85.7
Pollen tube	4	1	5	10.4
Pollen tube tip	0	1	1	8.3

Percentage* (%): DEGs related to pollen development/count of all background genes annotated to the GO category.

3.5. Characterization of the pectin methylesterase inhibitor gene *AtPMEI-pi*

AtPMEI-pi is located on chromosome 4 of *Arabidopsis*. The full length of *AtPMEI-pi* is 1097 bp, including two exons and one intron. The full length cDNA sequence is 767 bp with 67 bp 5' UTR and 184 bp 3' UTR, which can encode 171 amino acids. The relative molecular mass of AtPMEI-pi is 19.3 kD, the isoelectric point is 4.91, and the instability coefficient of AtPMEI-pi is 34.06 (less than 40)，indicating that it belongs to stable protein. The signal peptide of AtPMEI-pi is a 20 amino acid sequence located at the N-terminal of AtPMEI-pi, which has a splicing site at the 20-21 amino acid (TRA-DE) position (Fig. 5A). AtPMEI-pi has no transmembrane domain, indicating that it is a protein in cytoplasm or organelle, not a membrane protein or secretory protein (Fig. 5B). The recombinant plasmid *CaMV35S::AtPMEI-pi-GFP* was constructed and transferred into onion epidermal cells by microprojectile bombardment. Since pectin is the main component of the cell wall, plasmolysis of onion epidermis was carried out to determine whether *AtPMEI-pi* was expressed the cell wall. The fluorescence signal of the PMEI-GFP fusion protein was different from that of the positive control *CaMV35S::GFP*, which was present in both the nucleus and cytoplasm (Fig. 5C). The fluorescence signals showed that *AtPMEI-pi* was expressed mainly in the cytoplasm but not in the cell wall (Fig. 5D).

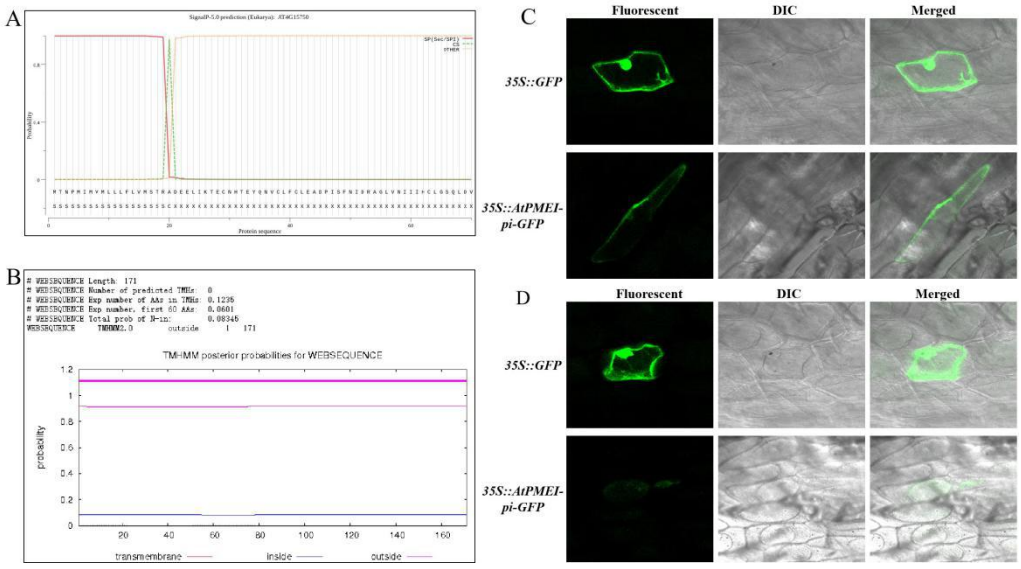

Fig. 5. Characteristics of pectin methylesterase inhibitor AtPMEI-pi. (A) Signal peptide analysis of AtPMEI-pi by SignalP-5.0. (B) Transmembrane domain analysis of AtPMEI-pi by TMHMM (http://www.cbs.dtu.dk/services/TMHMM/). (C) Subcelluar localization of AtPMEI-pi in onion epidermal cells. (D) Transient expression analysis of AtPMEI-pi in onion epidermal cells after plasmolysis.

3.6. Relative expression pattern of *AtPMEI-pi*

The transcripts of *AtPMEI-pi* in roots, seedlings, stems, leaves, flowers, and siliques of the WT,

eno2^{-}, and *mAtENO2-8* plants were detected by qRT-PCR. The relative expression levels of *AtPMEI-pi* in flowers and siliques were significantly higher than those in the other tissues. The relative expression level of *AtPMEI-pi* was 15-fold higher in the WT flowers than that in *eno2*$^{-}$ flowers, and 8461-fold higher than that in leaves of the WT flowers (Fig. 6A). The expression level of *AtPMEI-pi* was 320-fold higher in pollen than in flower buds and twice that in flowers (Fig. 6B), indicating that *AtPMEI-pi* was highly expressed in pollen, especially at later stages of pollen development. Since PMEI can directly affect the activity of PME, we analyzed the activity of PME in the pollen of the WT, *eno2*$^{-}$, and *mAtENO2-8*. The PME activity was higher in *eno2*$^{-}$ than in the WT and *mAtENO2-8* plants (Fig. 6C).

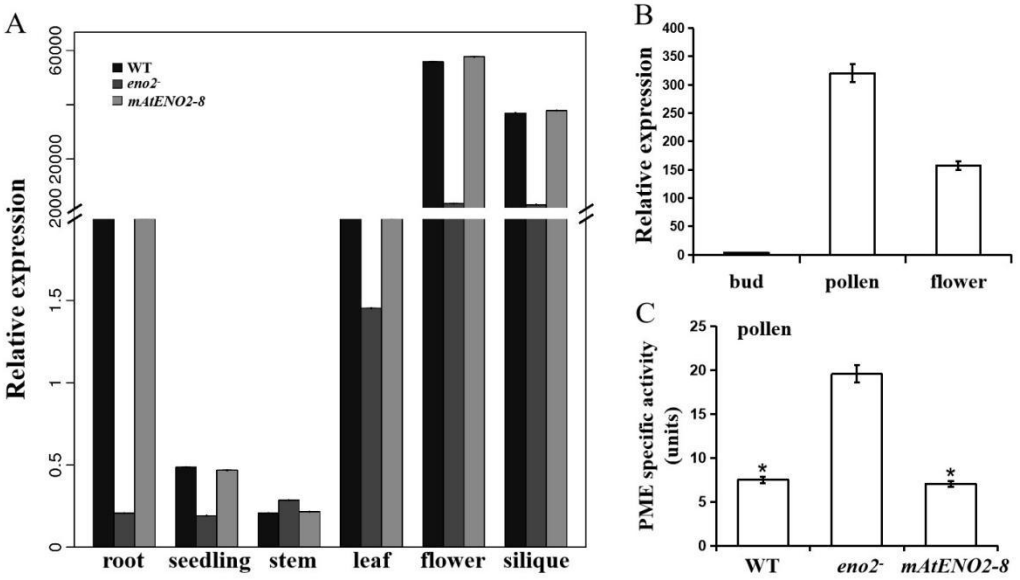

Fig. 6. Relative expression pattern of *AtPMEI-pi* and PME activity analysis. (A) Relative expression pattern analysis of *AtPMEI-pi* using qRT-PCR in different tissues of the WT, *eno2*$^{-}$, and *mAtENO2-8*. (B) Relative expression patterns of *AtPMEI-pi* in the bud, flower, and pollen of the WT. (C) PME activity in flowers of the WT, *eno2*$^{-}$, and *mAtENO2-8*. All experiments were performed in triplicate. Asterisks indicate a significant difference from *eno2*$^{-}$ ($P < 0.05$).

3.7. Functions of AtENO2 on formation of the pollen intine in *Arabidopsis*

According to the characteristics and relative expression pattern of *AtPMEI-pi*, to determine the effect of AtENO2 on the pollen intine, the morphology of pollen intine was observed. Transverse sections of pollen at the trinucleate stage were observed by transmission electron microscopy (TEM). Compared with the WT, the intine of the *mAtENO2-8* line was further thickened, whereas the intine of *eno2*$^{-}$ was seriously defective, showing a variety of defective phenotypes, such as abnormal thinning, abnormal thickening and deletion (Fig. 7). According to these results, we confirmed that AtENO2 could affect formation of the pollen intine in *Arabidopsis*.

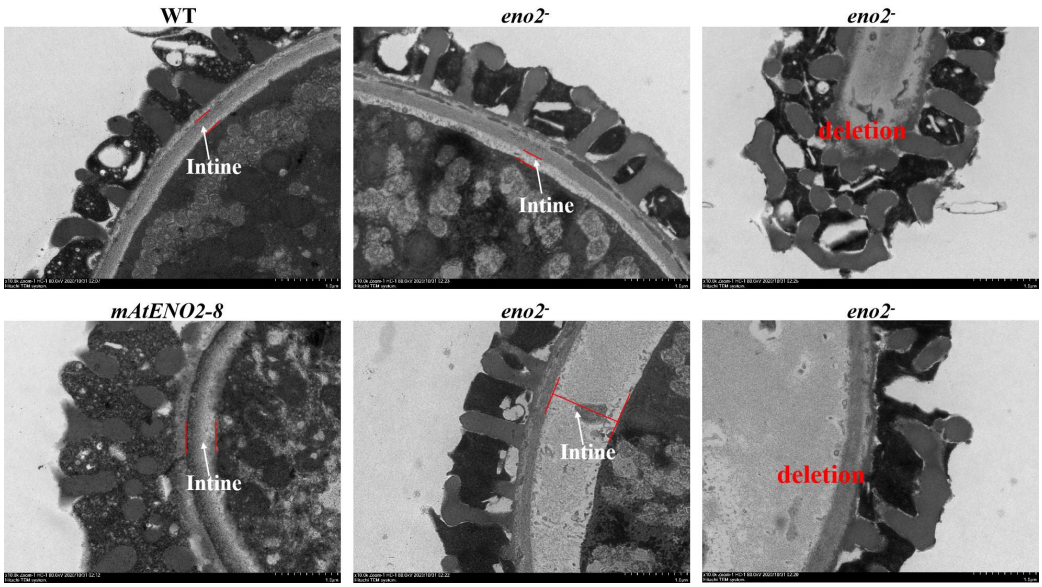

Fig. 7. Effect of AtENO2 on formation of the pollen intine layer. Transmission electron microscopy (TEM) of pollen at the trinucleate stage of the WT, *eno2*$^{-}$, and *mAtENO2-8*. Arrows indicate the pollen intine layer. the bars are 1.0 μm.

3.8. Functions of AtENO2 on the pollen germination and pollen tube growth.

Pectin is an important component of pollen tube wall, especially the top of pollen tube has only one layer of pectin wall. To determine the effect of AtENO2 on the pollen germination and pollen tube growth, the pollen germination rate and pollen tube growth were analyzed. The pollen germination rate of *eno2*$^{-}$ was lower than that of the WT, and the growth of the pollen tube was also defective. Compared with the WT, the pollen germination rate of *mAtENO2-8* line was higher and the growth of pollen tube was stronger (Fig. 8).

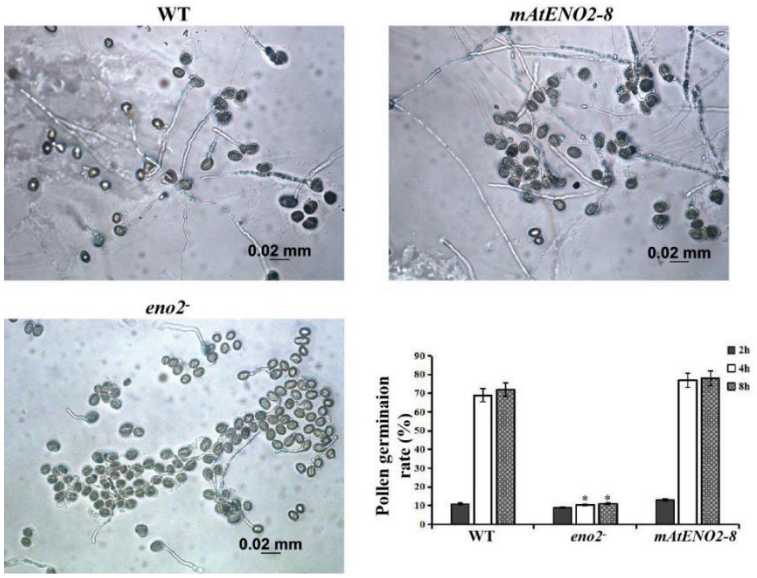

Fig. 8. Effect of AtENO2 on the pollen germination and pollen tube growth. Pollen germination in agar medium for the WT, *eno2*$^{-}$, and *mAtENO2-8 in vitro*. Asterisks indicate a significant difference from the WT ($P < 0.05$).

3.9. Effect of *AtENO2* on pollen development at the transcriptional level

Analysis of the 5′ terminal truncated of the *AtENO2* promoter revealed a significant difference in *GUS* gene expression between the *WT/AtENO2prom-734::GUS* and *WT/AtENO2prom-573::GUS* lines (Fig. 9A). The GUS activity was significantly higher in the anthers and stigmas of the *WT/AtENO2prom-734::GUS* line than the *WT/AtENO2prom-573::GUS* line ($P < 0.05$) (Fig. 9B). These results indicated that the -734 to -573 region of the *AtENO2* promoter was the main region of transcriptional regulation of *AtENO2* affecting flower and pollen development. Based on the PLACE database search (https://www.dna.affrc.go.jp/PLACE/?action=newplace), a pollen specific cis-element GTGANTG10(GTGA), involved in the region from -734 to -573 of the *AtENO2* promoter. Using the *AtENO2prom* (-734 ~ -573) sequence as a bait, yeast one-hybrid assay was carried out by using the transcription factor library. A total of 5 transcription factors related to floral organ development were screened (Fig. 9C).

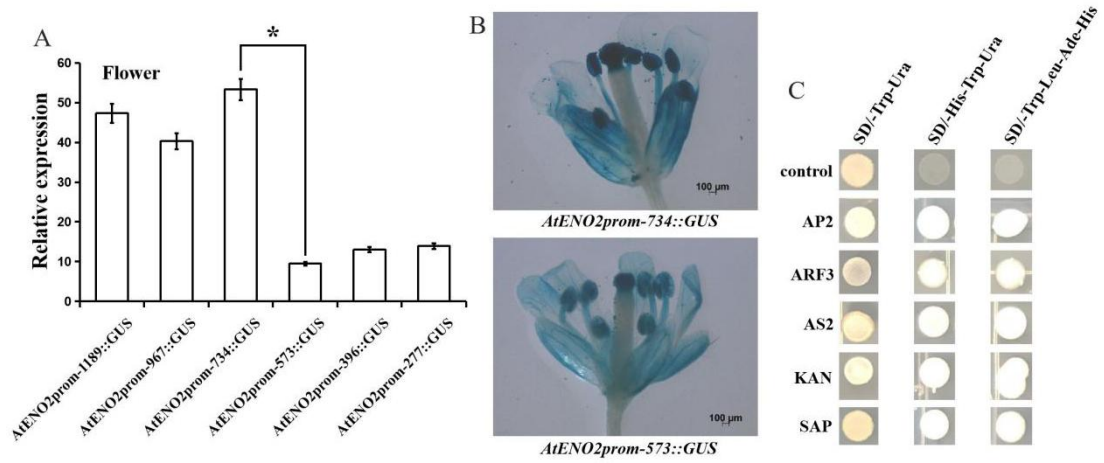

Fig. 9. Transcriptional analysis of *AtENO2* regulating pollen development. (A) Relative expression analysis of the *GUS* gene using qRT-PCR in the flower of transgenic plants with the truncated promoter sequences. The experiment was performed in triplicate ($P < 0.05$). (B) Histochemical GUS assay of the transgenic plants flowers. The flowers were randomly selected and treated under the same conditions. (C) The screening of transcription factors interacting with *AtENO2prom* (-734 ~ -573) by yeast one-hybrid.

4. Discussion

Double fertilization is an important biological process that directly affects the seed setting rate and seed yield. During double fertilization, pollen fertility is an important factor affecting the seed setting rate and crop yield (Moles *et al*., 2005; Dresselhaus and Franklin-Tong, 2013; Liu *et al*., 2016). In recent years, it has been found that *AtENO2* has an effect on pollen development. Compared with WT *Arabidopsis*, the pollen morphology, pollen germination rate *in vitro,* and pollen tube length of *eno2*$^{-}$ were all defective (Eremina *et al*., 2015; Liu *et al*., 2019). Enolase ENO2 is a key glycolytic enzyme that is widely distributed and highly conserved in plants. In addition to participating in the glycolytic pathway, recent studies have shown that the *ENO2* gene also has many non-glycolytic functions, such as affecting plant growth and responding to abiotic stresses (Lee *et al*., 2002; Barkla *et al*., 2009; Sharma *et al*., 2012; Kang *et al*., 2013; Eremina *et al*., 2015; Zhang *et al*., 2018; Liu *et al*., 2019, 2020). *AtENO2* encodes two proteins AtENO2 and AtMBP-1. Compared with the non-glycolytic function of AtENO2, there are many studies on the

function of AtMBP-1. For example, AtMBP-1 has a negative transcriptional regulation function and responds to abiotic stresses such as low temperature, ABA, and high salt, and feedback represses the activity of AtENO2 (Kang *et al*., 2013; Eremina *et al*., 2015; Liu *et al*., 2018b). However, the phenotypic analysis of the *eno2*$^{-}$*/35S::AtMBP-1-GFP* line showed that AtMBP-1 had no significant effect on the growth and development of *Arabidopsis* (Liu *et al*., 2019). Therefore, AtENO2 protein may be the main factor affecting the growth and development of *Arabidopsis*. In this study, through site-directed mutagenesis of the start codon of the AtMBP-1 coding sequence, we obtained a sequence that only expressed AtENO2 and obtained complementary transgenic lines (*eno2*$^{-}$*/35S::mAtENO2-GFP-5* and *eno2*$^{-}$*/35S::mAtENO2-GFP-8*) (Fig. 1B). Further analysis of the pollen development and morphology of the transgenic lines confirmed that AtENO2 had an important effect on the pollen development (Fig. 2).

PMEI can affect the pectin methyl esterification in the pollen intine by negatively regulating the activity of PME (Giovane *et al*., 2004; Matteo *et al*., 2005). Seventy-nine PMEI genes have been identified in *Arabidopsis* (Pinzón-Latorre *et al*., 2013). It was found that PMEI family genes have a variety of biological functions, such as affecting plant growth, organ development, fruit ripening and response to stresses (Pelletier *et al*., 2010; Peaucelle *et al*., 2015; Tundo *et al*., 2016; Liu *et al*., 2017). In this study, the gene with the highest significant expression difference was found by transcriptome sequencing. It was a *PMEI* family gene, *AtPMEI-pi* (*At4G15750*), with an unknown specific function. Multiple sequence alignment (Fig. 4C), tertiary structure prediction (Fig. 4D) and subcellular localization (Fig. 5C, D) of AtPMEI-pi indicated that AtPMEI-pi might be a cytoplasmic protein with PMEI activity. Furthermore, it was found that the expression level of *AtPMEI-pi* was the highest in *Arabidopsis* pollen, and the PME activity of *eno2*$^{-}$ mutant pollen was significantly higher than that of WT and *mAtENO2-8* (Fig. 6). These studies showed that AtENO2 may affect the development of pollen intine by regulating the expression of *AtPMEI-pi*. Transmission electron microscopy of pollen showed that AtENO2 did affect the pollen intine development. At present, we have confirmed that AtENO2 has an effect on development of the pollen intine, and its mechanism may be related to *AtPMEI-pi*. Only by verifying the PMEI activity of AtPMEI-pi at the protein level, obtaining double mutant of *eno2*$^{-}$ and *atpmei-pi*, or overexpression lines of *AtPMEI-pi*, can we make clear that the mechanism of AtENO2 in pollen intine development is indeed related to *AtPMEI-pi*.

PMEI can inhibit the activity of PME by non covalent binding with PME (Di Matteo *et al*., 2005). It has been found that the PMEI-PME interaction in *Arabidopsis* include AtPMEI2-AtPPME1, AtPMEI7-AtPME3, and AtPMEI4-AtPME17 (Röckel *et al*., 2008; Sénéchal *et al*., 2015). The *VGDH2* and *PME48* can affect pollen germination and pollen tube growth (Jiang *et al*., 2005; Leroux *et al*., 2015), but there is no report about PMEI inhibiting its activity. Because *AtPMEI-pi*, *VGDH2,* and *PME48* were significantly differentially expressed genes in *mAtENO2-8* vs. *eno2*$^{-}$ (Fig. 4A), whether AtPMEI-pi can inhibit the activity of VGDH2 or PME48 needs to be verified by protein interaction analysis. In addition, besides *VGDH2* and *PME48*, DEGs related to pectin metabolism also include *PME42*, *PME17*, *QRT1*, and *PME19*. Among them, *PME42*, *QRT1*, and *PME19* are expressed mainly in flowers and seeds. Whether AtPMEI-pi can regulate these genes needs further exploration.

The activity of the 5′ terminal truncated sequences of *AtENO2* promoter were analyzed. The results showed that the activity of *AtENO2*prom-734 in flowers was significantly higher than that of *AtENO2prom-573* (Fig. 9A). The GUS activity in anthers and stigmas of the two transgenic

Arabidopsis was also significantly different, which may be the difference of GUS activity in pollen. A pollen development specific element GTGANTG10 (GTGA) was found in the -734 ~ -573 (161 bp) sequence of *AtENO2* promoter. The element was first found in *g10*, a functional gene of tobacco pollen development. *g10* is homologous with *LAT56*, a specific gene of tomato pollen development. The homologous pollen specific genes *g10*, *LAT56*, *LAT52*, and *LAT59* are all pectate lyase homologous genes, and GTGA element is a common element in the promoters of these genes. Through mutation and deletion analysis of GTGA element in *g10* promoter, it was found that GTGA element was a functional element affecting pollen development (McCormick *et al*., 1991; Kim *et al*., 1997; Rogers *et al*., 2001). Whether this element is a functional element of AtENO2 affecting pollen development remains to be studied. The main function of pectate lyase (PL) is to degrade demethyl-esterified pectin by PME. Pectate lyase-like genes catalyze the degradation of pectin in the presence of Ca^{2+} through β-elimination. They are necessary for loosening of the pollen intine and entry of the pollen tube into the style during pollen germination (Youssef and Anja, 2018). Demethyl esterification of pectin reduced the pH value, and low pH affected the activity of pectate lyase and the plasticity of the pollen wall. The dynamic balance among PMEI, PME, and PL is important to maintain the metabolism of pectin (Catoire *et al.*, 1998; Denès *et al.*, 2000; Chebli *et al*., 2012; Wang *et al*., 2020). Therefore, it is necessary to explore whether the relationship between AtENO2 and AtPMEI-pi is related to pectate lyase. Transcription factors KAN, AS2, and ARF3/ETT could interact with the -734 ~ -573 sequence of *AtENO2* promoter (Fig. 9C). The organ polarity gene *KAN* plays an important role in leaf, carpel and flower organs (Ó'Maoiléidigh *et al*., 2018; Zumajo-Cardona and Ambrose, 2020). KAN can directly inhibit the expression of *AS2*, and AS2 can directly participate in the epigenetic inhibition of *ARF3* through DNA methylation (Wu *et al*., 2008; Machida *et al*., 2015; Vial-Pradel *et al*., 2018). ARF3 is a transcription factor of ARF (Auxin response factor) family. ARF3 affects floral meristem development by regulating cytokinin biosynthesis and signal transduction. ARF3 is also correlates with a reduction in the methylesterification of cell-wall pectins and a decrease in cell-wall stiffness in the valve tissues of the ovary (Zheng *et al*., 2018; Andres-Robin *et al*., 2020). Immediate targets of ARF3 suggest PMEIs are likely to be key actors that mediate the regulation of gynecium development by ARF3, while ARF3 may simultaneously regulate PMEs to prevent exaggerated developmental effects from the regulation of PMEIs. In addition, there are one or more rapidly-acting intermediate factors in the transcriptional regulation of PMEs and PMEIs by ARF3 (Andres-Robin *et al*., 2020). Whether these transcription factors are involved in the regulatory mechanism of AtENO2 affecting pollen development needs to be verified by DNA-protein interaction and analysis of deletion mutants of the transcription factors. We constructed a model of AtENO2 on development of the pollen intine based on the current results together with previous findings (Fig. 10).

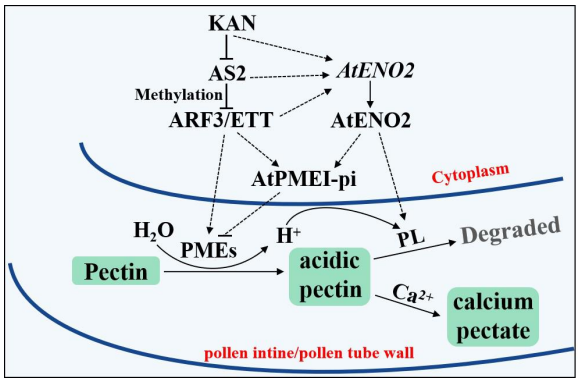

Fig. 10. The regulatory network of AtENO2 in pollen intine development.

Compared with the pollen intine, the structure of pollen exine is more complex. The exine is further divided into the sexine layer and nexine layer (Hesse *et al.,* 2016; Paxson-Sowders *et al.,* 2001). The pollen exine is mainly composed of tectum, bacula and footlayer, but some pollen walls have no tectum (Shi *et al.,* 2015). These structures can form species-specific textures on the pollen surface. The chemical composition of the exine is mainly sporopollenin, which has extreme corrosion resistance. In *Arabidopsis* and other plants, the pollen coat is also attached to the pollen exine, such as tryphine or pollenkitt, which are mainly composed of lipids, proteins, pigments and aromatic compounds that are crucial for the recognition of pollen fertilization signals and the attachment of stigmas. The nexine is a smooth cell wall located on the surface of the intine, which is divided into two layers: nexine I and nexine II (Ariizumi and Toriyama, 2012). In this study, the pollen exine structure of *mAtENO2-8* was denser than that of *eno2*$^{-}$ by TEM. In addition, it was found that the pollen nexine of *eno2*$^{-}$ was thickened or completely absent (Fig. 7). Transcriptome analysis of the *eno2*$^{-}$ and *mAtENO2-8* lines revealed that many DEGs related to development of the pollen exine and pollen coat, such as *AMS*, *MS1*, *ABCG1/26*, *CYP703A2*, *CYP704B1*, *PKSA/B*, and *TKRP1/2*. The genetic pathway DYT1-TDF1-AMS-MS188/MS103-MS1 controls pollen exine formation by regulating sporopollen synthesis and transport. AMS and MS1 are important transcription factors in this pathway (Shi *et al*., 2015; Lu *et al*., 2020). AMS can also directly regulate the expression of *TEK*, forming DYT1-TDF1-AMS-TEK genetic pathway to regulate formation of the pollen nexine (Xiong *et al*., 2016; Wang *et al*., 2018). ABCG1/26 are transporters of the sporopollen, while *CYP703A2*, *CYP704B1*, *PKSA/B*, and *TKRP1/2* are the genes involved in sporopollen biosynthesis in tapetum (Morant *et al*., 2007; de Azevedo Souza *et al*., 2009; Grienenberger *et al*.,2010; Kim *et al*., 2010; Chen *et al*., 2011). These finding indicates that AtENO2 plays an important role in regulating development of the pollen exine, although the regulatory mechanism remains unclear.

5. Conclusion

AtENO2 can affect pollen development and encode two proteins AtENO2 and AtMBP-1. We obtained the sequence encoding only AtENO2 and studied the functions and molecular mechanisms of AtENO2 in pollen development. The results presented herein show that AtENO2 can affect development of the pollen intine, and the mechanism may be that AtENO2 regulated the methyl esterification of pectin in pollen intine through ARF3 and AtPMEI-pi. The -734 ~ -573 sequence of *AtENO2* promoter is the main transcriptional regulatory region of AtENO2 affecting pollen development. The functional cis-acting element may be GTGANTG10(GTGA), and the

trans-acting factors may be KAN, AS2 and ARF3. Moreover, the deletion of AtENO2 can cause significant difference in the expression of multiple genes related to pollen exine development.

CRediT authorship contribution statement

Xiaofeng Ma: Conceptualization, Methodology, Software, Validation, Writing - original draft. **Yu Wu:** Data curation, Methodology, Writing - review & editing. **Huimin Liu:** Investigation. **ZiJin Liu:** Validation. **Hongjie Li:** Writing - review & editing. **Genfa Zhang:** Supervision, Project administration, Funding acquisition.

Declaration of Competing Interest

The authors report no declarations of interest.

Acknowledgments

This work was supported by the National Natural Science Foundation of China (31872672 and 31470399).

References

Andres-Robin, A., Reymond, M.C., Brunoud, G., Martin-Magniette, M.L., Monéger, F., Scutt, C.P., 2020. Immediate targets of ETTIN suggest a key role for pectin methylesterase inhibitors in the control of *Arabidopsis* gynecium development. *Plant Signal Behav*. 15, 1771937.

Aouali, N., Laporte, P., Clément, C., 2001. Pectin secretion and distribution in the anther during pollen development in *Lilium*. *Planta* 213, 71-79.

Ariizumi, T., Hatakeyama, K., Hinata, K., Inatsugi, R., Nishida, I., Sato, S., Kato, T., Tabata, S., Toriyama, K., 2004. Disruption of the novel plant protein NEF1 affects lipid accumulation in the plastids of the tapetum and exine formation of pollen, resulting in male sterility in *Arabidopsis thaliana*. *Plant J*. 39, 170-181.

Ariizumi, T., Toriyama, K., 2012. Genetic regulation of sporopollenin synthesis and pollen exine development. *Annual Review of Plant Biology* 62, 437-460.

Barkla, B.J., Vera-Estrella, R., Hernández-Coronado, M., Pantoja, O., 2009. Quantitative proteomics of the tonoplast reveals a role for glycolytic enzymes in salt tolerance. *Plant Cell* 21, 4044-4058.

Bosch, M., Cheung, A.Y., Hepler, P.K., 2005. Pectin methylesterase, a regulator of pollen tube growth. *Plant Physiol*. 138, 1334-1346.

Catoire, L., Pierron, M., Morvan, C., Goldberg, R., 1998. Investigation of the action patterns of pectin methylesterase isoforms through kinetic analyses and NMR spectroscopy. Implications in cell wall expansion. *J Biol Chem*. 273, 33150-33156.

Chen, W.W., Yu, X.H., Zhang, K.S., Shi, J.X., Oliveira, S.D., Schreiber, L., Shanklin, J., Zhang, D., 2011. Male Sterile2 encodes a plastid-localized fatty acyl carrier protein reductase required for pollen exine development in *Arabidopsis. Plant Physiol*. 157, 842-853.

Chebli, Y., Kaneda, M., Zerzour, R., Geitmann, A., 2012. The cell wall of the *Arabidopsis* pollen tube--spatial distribution, recycling, and network formation of polysaccharides. *Plant Physiol*. 160, 1940-1955.

Dardelle, F., Lehner, A., Ramdani, Y., Bardor, M., Lerouge, P., Driouich, A., Mollet, J.C., 2010. Biochemical and immunocytological characterizations of *Arabidopsis* pollen tube cell wall. *Plant Physiol*. 153, 1563-1576.

de Azevedo Souza, C., Kim, S.S., Koch, S., Kienow, L., Schneider, K., McKim, S.M., Haughn, G.W., K ombrink, E., Douglas, C.J., 2009. A novel fatty acyl-CoA synthetase is required for pollen developm ent and sporopollenin biosynthesis in *Arabidopsis*. *Plant Cell* 21, 507-525.

Dedeurwaerder, S., Bouaouiche, L.M., Mareck, A., Lerouge, P., Guerineau, F., 2009. Activity of an atypical *Arabidopsis thaliana* pectin methylesterase. *Planta* 229, 311-321.

Denès, J.M., Baron, A., Renard, C.M., Péan, C., Drilleau, J.F., 2000. Different action patterns for apple pectin methylesterase at pH 7.0 and 4.5. *Carbohydr Res*. 327, 385-393.

Di Matteo, A., Giovane, A., Raiola, A., Camardella, L., Bonivento, D., de Lorenzo, G., Cervone, F., Bellicampi, D., Tsernoglou, D., 2005. Structural basis for the interaction between pectin methylesterase and a specific inhibitor protein. *Plant Cell* 17, 849-858.

Dresselhaus, T., Franklin-Tong, N., 2013. Male-female crosstalk during pollen germination, tube growth and guidance, and double fertilization. *Mol Plant*. 6, 1018-1036.

Eremina, M., Rozhon, W., Yang, S., Poppenberger, B., 2015. ENO2 activity is required for the development and reproductive success of plants, and is feedback-repressed by AtMBP-1. *Plant J*. 6, 895-906.

Gigli, N.B., Savatin, D.V., Cervone, F., Engelsdorf, T., Lorenzo, G.D., 2018. Loss of the *Arabidopsis* protein kinases ANPs affects root cell wall composition, and triggers the cell wall damage syndrome. *Front Plant Sci*. 8, 2234.

Giovane, A., Servillo, L., Balestrieri, C., Raiola, A., Avino, R., Tamburrini, M., Ciardiello, M.A., Camardella, L., 2004. Pectin methylesterase inhibitor. *Biochim Biophys Acta*. 1696, 245-252.

Grienenberger, E., Kim, S.S., Lallemand, B., Geoffroy, P., Heintz, D., de Azevedo Souza, C., Heitz, T., Douglas, C.J., Legrand, M., 2010. Analysis of TETRAKETIDE α-PYRONE REDUCTASE function in *Arabidopsis thaliana* reveals a previously unknown but conserved, biochemical pathway in sporopoll enin monomer biosynthesis. *Plant Cell* 22, 4067-4083.

Guan, Y.F., Huang, X.Y., Zhu, J., Gao, J.F., Zhang, H.X., Yang, Z.N., 2008. RUPTURED POLLEN GRAIN1, a member of the MtN3/saliva gene family, is crucial for exine pattern formation and cell integrity of microspores in *Arabidopsis*. *Plant Physiol*. 147, 852-863.

Hesse, U.M., Halbritter, H., Zetter, R., Weber, M., Buchner, R., Frosch-Radivo, A., Ulrich, S., 2016. Pollen and Spore Terminology. Springer Vienna.

Jiang, L.X., Yang, S.L., Xie, L.F., Puah, C.S., Zhang, X.Q., Yang, W.C., Sundaresan, V., Ye, D., 2005. VANGUARD1 encodes a pectin methylesterase that enhances pollen tube growth in the *Arabidopsis* style and transmitting tract. *Plant Cell* 17, 584-596.

Kang, M., Abdelmageed, H., Lee, S., Reichert, A., Mysore, K.S., Allen, R.D., 2013. AtMBP-1, an alternative translation product of LOS2, affects abscisic acid responses and is modulated by the E3 ubiquitin ligase AtSAP5. *Plant J*. 76, 481-493.

Kim, H.U., Park, B.S., Jin, Y.M., Chung, T.Y., 1997. Promoter sequences of two homologous pectin esterase genes from Chinese cabbage (Brassica campestris L. ssp. pekinensis) and pollen-specific expression of the GUS gene driven by a promoter in tobacco plants. *Mol Cells*. 7, 21-27.

Kim, S.S., Grienenberger, E., Lallemand, B., Colpitts, C.C., Kim, S.Y., Heintz, D., Krahn, D., Kaiser, M., Kombrink, E., Douglas, C.J., 2010. *LAP6/POLYKETIDE SYNTHASE A* and *LAP5/POLYKETIDE SYN THASE B* encode hydroxyalkyl α-pyrone synthases required for pollen development and sporopolleni n biosynthesis in *Arabidopsis thaliana. Plant Cell* 22, 4045-4066.

Lee, H., Guo, Y., Ohta, M., Xiong, L.M., Stevenson, B., Zhu, J.K., 2002. LOS2, a genetic locus required for cold-responsive gene transcription encodes a bi-functional enolase. *EMBO J*. 21, 2692-2702.

Leroux, C., Bouton, S., Meyer, M.K., Fabrice, T.N., Mareck, A., Guenin S., Fournet, F., Ringli, C., Pelloux, J., Driouich, A., Lerouge, P., Lehner, A., Mollet, J., 2015. PECTIN METHYLESTERASE48 is involved in *Arabidopsis* pollen grain germination. *Plant Physiol*. 167, 367-380.

Lionetti, V., Fabri, E., De Caroli, M., Hansen, A.R., Willats, W.G.T., Piro, G., Bellincampi, D., 2017. Three pectin methylesterase inhibitors protect cell wall integrity for immunity to *Botrytis*. *Plant Physiol*. 173, 1844-1863.

Liu, C.Q., Hu, K.D., Li, T.T., Yang, Y., Yang, F., Li, Y.H., Liu, H.P., Chen, X.Y., Zhang, H., 2017. Polygalacturonase gene *pgxB* in *Aspergillus niger* is a virulence factor in apple fruit. *PLoS One* 12, eO173277.

Liu, N.N., Sun, Y., Pei, Y.K., Zhang, X.Y., Wang, P., Li, X.C., Li, F.G., Hou, Y.X., 2018a. A pectin methylesterase inhibitor enhances resistance to *Verticillium* wilt. *Plant Physiol*. 176, 2202-2220.

Liu, K.G., Qi, S.H., Li, D., Jin, C.Y., Gao, C.H., Duan, S.W., Feng, B.L., Chen, M.X., 2016. TRANSPARENT TESTA GLABRA 1 ubiquitously regulates plant growth and development from *Arabidopsis* to foxtail millet (*Setaria italica*). *Plant Sci*. 254, 60-69.

Liu, Z.J., Zhang, A., Zheng, L.M., Johnathan, A.F., Zhang, J., Zhang, G.F., 2018b. The Biological Signifi cance and Regulatory Mechanism of c-Myc Binding Protein 1 (MBP-1). *Int J Mol Sci*. 19, 3868.

Liu, Z.J., Zhang, Y.H., Ma, X.F., Ye, P., Gao, F., Li, X.F., Zhou, Y.J., Zheng, C.X., Li, H.J., Zhang, G.F., 2019. Biological functions of *Arabidopsis thaliana* MBP-1-like protein encoded by ENO2 in the response to drought and salt stresses. *Physiol Plant*. 168, 660-674.

Liu, Z.J., Zheng, L.M., Li, P., Ma, X.F., Wang, X., Wu, Y., Ming, H.N., Wang, Q., Zhang, G.F., 2020. ENO2 affects the seed size and weight by adjusting cytokinin content and forming ENO2-bZIP75 complex in *Arabidopsis thaliana*. *Front Plant Sci*. 26, 11:574316.

Lu, J.Y., Xiong, S.X., Yin, W.Z., Teng, X.D., Lou, Y., Zhu, J., Zhang, C., Gu, J.N., Yang, Z.N., 2020. MS1, a direct target of MS188, regulates the expression of key sporophytic pollen coat protein genes in *Arabidopsis*. *J Exp Bot*. 71, 4877-4889.

Matteo, A.D., Giovane, A., Raiola, A., Camardella, L., Bonivento, D., Lorenzo, G.D., Cervone, F., Bellincampi, D., Tsernoglou, D., 2005. Structural basis for the interaction between pectin methylesterase and a specific inhibitor protein. *Plant Cell* 17, 849-858.

Machida, C., Nakagawa, A., Kojima, S., Takahashi, H., Machida, Y., 2015. The complex of ASYMMETRI C LEAVES (AS) proteins plays a central role in antagonistic interactions of genes for leaf polarity s pecification in Arabidopsis. *Wiley Interdiscip Rev Dev Biol*. 4, 655-671.

McCormick, S., Twell, D., Vancanneyt, G., Yamaguchi, J., 1991. Molecular analysis of gene regulation a nd function during malegametophyte development. *Symp Soc Exp Biol*. 45, 229-244.

Mohnen, D., 2008. Pectin structure and biosynthesis. *Curr Opin Plant Biol*. 11, 266-277.

Moles, A.T., Ackerly, D.D., Webb, C.O., Tweddle, J.C., Dickie, J.B., Pitman, A.J., Westoby, M., M.W., 2005. Factors that shape seed mass evolution. *Proc Natl Acad Sci USA*. 102, 10540-10544.

Morant, M., Jørgensen, K., Schaller, H., Pinot, F., Møller, B.L., Werck-Reichhart, D., Bak, S., 2007. CY P703 is an ancient cytochrome P450 in land plants catalyzing in-chain hydroxylation of lauric acid t o provide building blocks for sporopollenin synthesis in pollen. *Plant Cell* 19, 1473-1487.

Nguyen, H.P., Jeong, H.Y., Kim, H., Kim, Y.C., Lee, C.H., 2016. Molecular and biochemical characterization of rice pectin methylesterase inhibitors (OsPMEIs). *Plant Physiol Biochem*. 101, 105-112.

Paxson-Sowders, D.M., Dodrill, C.H., Owen, H.A., Makaroff, C.A., 2001. DEX1, a novel plant protein, is required for exine pattern formation during pollen development in *Arabidopsis. Plant Physiol*. 127, 1739-1749.

Paynel, F., Leroux, C., Surcouf, O., Schaumann, A., Pelloux, J., Driouich, A., Mollet, J.C., Lerouge, P., Lehner, A., Mareck, A., 2014. Kiwi fruit PMEI inhibits PME activity, modulates root elongation and induces pollen tube burst in *Arabidopsis thaliana*. *Plant Growth Regul*. 74, 285-297.

Peaucelle, A., Louvet, R., Johansen, J.N., Hofte, H., Laufs, P., Pelloux, J., Mouille, G., 2008. *Arabidopsis* phyllotaxis is controlled by the methyl-esterification status of cell-wall pectins. *Curr Biol*. 18, 1943-1948.

Peaucelle, A., Wightman, R., Hofte, H., 2015. The Control of growth symmetry breaking in the *Arabidopsis* hypocotyl. *Curr Biol*. 25, 1746-1752.

Pelletier, S., Orden, J.V., Wolf, S., Vissenberg, K., Delacourt, J., Renou, J.P., Hofte, H., 2010. A role for pectin de-methylesterification in a developmentally regulated growth acceleration in dark-grown *Arabidopsis* hypocotyls. *New Phytol*. 188, 726-739.

Pelloux, J., Rustérucci, C., Mellerowicz, E.J., 2007. New insight into pectin methylesterase structure and function. *Trends Plant Sci*. 12, 267-277.

Pinzón-Latorre, D., Deyholos, M.K., 2013. Characterization and transcript profiling of the pectin methylesterase (PME) and pectin methylesterase inhibitor (PMEI) gene families in flax (*Linum usitatissimum*). *BMC Genomics* 14, 742.

Ó'Maoiléidigh, D.S., Stewart, D., Zheng, B.B., Coupland, G., Wellmer, F., 2018. Floral homeotic proteins modulate the genetic program for leaf development to suppress trichome formation in flowers. *Development* 145, dev157784.

Quilichini, T.D., Grienenberger, E., Douglas, C.J., 2015. The biosynthsis, composition and assembly of the outer pollen wall: a tough case to crack. *Phytochemistry* 113, 170-182.

Ridley, B.L., O'Neill, M.A., Mohnen, D., 2001. Pectins: structure, biosynthesis, and oligogalacturonide-related signaling. *Phytochemistry* 57, 929-967.

Röckel, N., Wolf, S., Kost, B., Rausch, T., Greiner, S., 2008. Elaborate spatial patterning of cell-wall PME and PMEI at the pollen tube tip involves PMEI endocytosis, and reflects the distribution of esterified and de-esterified pectins. *Plant J*. 53, 133-143.

Rogers, H.J., Bate, N., Combe, J., Sullivan, J., Sweetman, J., Swan, C., Lonsdale, D.M., Twell, D., 2001. Functional analysis of cis-regulatory elements within the promoter of the tobacco late pollen gene *g10*. *Plant Mol Biol*. 45, 577-585.

Saez-Aguayo, S., Ralet, M.C., Berger, A., Botran, L., Ropartz, D., Marion-Poll, A., North, H.M., 2013. Pectin methylesterase inhibitor6 promotes *Arabidopsis* mucilage release by limiting methylesterification of homogalacturonan in seed coat epidermal cells. *Plant Cell* 25, 308-323.

Sanders, P.M., Bui, A.Q., Weterings, K., McIntire, K.N., Goldberg, R.B., 1999. Anther developmental defects in *Arabidopsis* thaliana male-sterile mutants. *Sexual Plant Reproduct* 11, 297-322.

Scott, R.J., Spielman, M., Dickinson, H.G., 2004. Stamen structure and function. *Plant Cell* 16, 46-60.

Sénéchal, F., L'Enfant, M., Domon,J.M., Rosiau, E., Crépeau, M.J., Kim, H.R., Mravec, J., Bonnin, E., Jamet, E., Kihara, D., Lerouge, P., Pelloux, J., Rayon, C., 2015. Tuning of pectin methylesterification: pectin methylesterase inhibitor 7 modulates the processive activity of co-expressed pectin methylesterase 3 in a ph-dependent manner. *J Biol Chem*. 290, 23320-23335.

Sharma, P., Ganeshan, P., Fowler, D.B., Chibbar, R., 2012. Characterisation of two wheat enolase cDNA showing distinct patterns of expression in leaf and crown tissues of plants exposed to low temperature. *Ann Appl Biol*. 162, 271-283.

Shi, J.X., Cui, M.H., Yang, L., Kim, Y.J., Zhang, D.B., 2015. Genetic and biochemical mechanisms of pollen wall development. *Trends Plant Sci*. 20, 741-753.

Solecka, D., Zebrowski, J., Kacperska, A., 2008. Are pectins involved in cold acclimation and de-acclimation of winter oil-seed rape plants? *Ann Bot*. 101, 521-530.

Straeten, D.V.D., Rodrigues-Pousada, R.A., Goodman, H.M., Montagu, M.V., 1991. Plant enolase: gene structure, expression, and evolution. *Plant Cell* 3, 719-735.

Tundo, S., Kalunke, R., Janni, M., Volpi, C., Lionetti, V., Bellincampi, D., Favaron, F., Ovidio, R., 2016. Pyramiding PvPGIP2 and TAXI-III but not PvPGIP2 and PMEI enhances resistance against *Fusarium graminearum*. *Mol Plant-Microbe Interact* 29, 629-639.

Varner, J.E., Lin, L.S., 1989. Plant cell wall architecture. *Cell* 56, 231-239.

Vial-Pradel, S., Keta, S., Nomoto, M., Luo, L.L., Takahashi, H., Suzuki, M., Yokoyama, Y., Sasabe, M., Kojima, K., Tada, Y., Machida, Y., Machida, C., 2018. *Arabidopsis* Zinc-Finger-Like Protein ASYMMETRIC LEAVES2 (AS2) and Two Nucleolar Proteins Maintain Gene Body DNA Methylation in the Leaf Polarity Gene ETTIN (ARF3). *Plant Cell Physiol*. 59, 1385-1397.

Wang, K., Guo, Z.L., Zhou, W.T., Zhang, C., Zhang, Z.Y., Lou, Y., Xiong, S.X., Yao, X.Z., Fan, J.J., Zhu, J., Yang, Z.N., 2018. The Regulation of Sporopollenin Biosynthesis Genes for Rapid Pollen Wall Formation. *Plant Physiol*. 178, 283-294.

Wang, X., Wilson, L., Cosgrove, D.J., 2020. Pectin methylesterase selectively softens the onion epidermal wall yet reduces acid-induced creep. *J Exp Bot*. 71, 2629-2640.

Willats, W.G., McCartney, L., Mackie, W., Knox, J.P., 2001. Pectin: cell biology and prospects for functional analysis. *Plant Mol Biol*. 47, 9-27.

Woriedh, M., Wolf, S., Márton, M.L., Hinze, A., Gahrtz, M., Becker, D., Dresselhaus, T., 2013. External application of gametophyte-specific ZmPMEI1 induces pollen tube burst in maize. *Plant Reproduct* 26, 255-266.

Wu, G., Lin, W.C., Huang, T.B., Poethig, S.R., 2008. Springer, P.S., Kerstetter, R.A., KANADI1 regulates adaxial-abaxial polarity in *Arabidopsis* by directly repressing the transcription of ASYMMETRIC LEAVES2. *Proc Natl Acad Sci USA*. 105, 16392-16397.

Xiong, S.X., Lu, J.Y., Lou, Y., Teng, X.D., Gu, J.N., Zhang, C., Shi, Q.S., Yang, Z.N., Zhu, J., 2016. The transcription factors MS188 and AMS form a complex to activate the expression of *CYP703A2* for sporopollenin biosynthesis in *Arabidopsis thaliana*. *Plant J.* 88, 936-946.

Youssef, C., Anja, G., 2018. FRAP experiments show pectate lyases promote pollen germination and lubricate the path of the pollen tube in *Arabidopsis thaliana*. *Microsc Microanal*. 24, 1376-1377.

Zhang, G.Y., Feng, J., Wu, J., Wang, X.W., 2010. BoPMEI1, a pollen-specific pectin methylesterase inhibitor, has an essential role in pollen tube growth. *Planta* 231, 1323-1334.

Zhang, Y.H., Chen, C., Shi, Z.H., Cheng, H.M., Bing, J., Ma, X.F., Zheng, C.X., Li, H.J., Zhang, G.F., 2018. Identification of salinity-related genes in ENO2 mutant (eno2^{-}) of *Arabidopsis thaliana*. *J Integr Agric*. 17, 94-110.

Zhang, Z.B., Zhu, J., Gao, J.F., Wang, C., Li, H., Li, H., Zhang, S., Wang, D.M., Xia, H.J., Yang, Z.N., 2007. Transcription factor AtMYB103 is required for anther development by regulating tapetum development, callose dissolution and exine formation in *Arabidopsis*. *Plant J*. 52, 528-538.

Zheng, Y., Zhang, K., Guo, L., Liu, X., Zhang, Z., 2018. AUXIN RESPONSE FACTOR3 plays distinct role during early flower development. *Plant Signal Behav*. 13, e1467690.

Zhu, L., He, S.Y., Liu, Y.Y., Shi, J.X., Xu, J., 2020. *Arabidopsis* FAX1 mediated fatty acid export is required for the transcriptional regulation of anther development and pollen wall formation. *Plant Mol Biol*. 104, 187-201.

Zumajo-Cardona, C., Ambrose, B.A., 2020. Phylogenetic analyses of key developmental genes provide insight into the complex evolution of seeds. *Mol Phylogenet Evol*. 147, 106778.